Broadband absorption enhancement in anisotropic metamaterials by mirror reflections

Jiong Yang,[1] Xinhua Hu,[2,3,*] Xin Li,[4] Zheng Liu,[5] Zixian Liang,[5] Xunya Jiang,[5] and Jian Zi[1,3]
[1]*Department of Physics and Surface Physics Laboratory, Fudan University, Shanghai 200433, People's Republic of China*
[2]*Department of Material Science, Fudan University, Shanghai 200433, People's Republic of China*
[3]*Laboratory of Advanced Materials, Fudan University, Shanghai 200433, People's Republic of China*
[4]*Polar Research Institute of China, Shanghai 200136, People's Republic of China*
[5]*State Key Laboratory of Functional Materials for Informatics, Shanghai Institute of Microsystem and Information Technology, Chinese Academy of Science, Shanghai 200050, People's Republic of China*
(Received 18 April 2009; revised manuscript received 15 July 2009; published 8 September 2009)

Nonresonant anisotropic metamaterials (AMMs), such as nanotube arrays, can be applied to achieve broadband absorption of electromagnetic (EM) waves. However, the AMMs should be very thick (~1000 wavelengths) to attain high absorption. Here, we propose that using a slanted or corrugated metallic mirror, a thin AMM (~3 wavelengths) is sufficient to obtain high absorption in a wide wavelength range (absorption >87% for wavelengths of 0.5–3 μm) and over a wide angular range. Unlike common absorptions, EM waves in an ambient medium (air) is first coupled with a propagating wave in the AMM and is then converted into a lossy wave by mirror reflections.

DOI: 10.1103/PhysRevB.80.125103 PACS number(s): 42.25.Bs, 78.68.+m, 78.20.Ci

Metamaterials (MMs), a class of artificial periodic structures, have received great interest due to their exotic electromagnetic (EM) properties.[1–21] Unlike photonic crystals, MMs have a period much smaller than the working wavelength and can be viewed as homogeneous media described by effective dielectric constant ε_e and effective magnetic permeability μ_e.[1] By including resonant elements,[2,3] ε_e and μ_e of MMs can be tailored of extreme value leading to fascinating phenomena such as negative refraction and superlensing.[4,5] Recently, anisotropic MMs (AMMs) have also attracted growing attention.[6–20] With stratified[7–9] or cylindrical[10,11] structures, AMMs can exhibit strong anisotropy where ε_e and μ_e become tensors and their elements can be even of opposite algebraic signs.[6–9] As a result, many interesting phenomena which are difficult to be realized by natural materials, such as Dyakonov surface waves,[12] hyperlensing,[13–15] and cloaking,[16–20] can be achieved.

The imaginary parts of ε_e and μ_e in MMs usually induce absorption which can make the above effects vague or even unobservable. On the other hand, the absorption properties of MMs can also be utilized if the structures are specially designed. Recently, an ultrathin MM board has been fabricated as a narrowband microwave absorber.[21] Using a resonant structure, EM waves can be absorbed nearly completely in a very short distance (about 1/35 of vacuum wavelength λ_0).[21,22] Nonresonant AMMs such as low-density nanotube arrays (where $\varepsilon_e \approx 1+pi$ and $p \ll 1$)[11] can be utilized to realize broadband absorption.[23] But the AMMs should be very thick ($\sim 1000\lambda_0$) to attain high absorption.

In this paper, we propose that using a slanted or corrugated metal mirror, the absorption in AMMs can be enhanced by 20 times in a wide frequency range. As a result, a thin AMM (thickness $\sim 4\lambda_0$) is sufficient to obtain broadband high absorption (absorption >87% for wavelengths of 0.5–3 μm). Unlike common absorptions, EM waves in an ambient medium is first coupled with a propagating wave in AMMs and is then converted into a lossy wave by mirror reflections.

To illustrate the principle, we adopt an AMM composed of periodic stacking of metallic and dielectric layers. The metal layers have a thickness d_1 and dielectric constant ε_1. The dielectric layers have a thickness d_2 and dielectric constant ε_2. $\mu=1$ for all the layers. The period $d=d_1+d_2$. The normal of the metallic layers is defined as the x axis. We consider p-polarized EM waves propagating in the x-z plane ($k_y=H_x=H_z=E_y=0$). Using a transfer-matrix method (TMM) and imposing the Bloch theorem, the dispersion can be derived for the p waves,[24,25]

$$\cos(k_x d) = \cos(q_{1x}d_1)\cos(q_{2x}d_2) - \frac{1}{2}\left(\eta + \frac{1}{\eta}\right)\sin(q_{1x}d_1)\sin(q_{2x}d_2), \quad (1)$$

where $(k_x,0,k_z)$ is the Bloch wave vector, $q_{1x}=\sqrt{\varepsilon_1 k_0^2 - k_z^2}$, $q_{2x}=\sqrt{\varepsilon_2 k_0^2 - k_z^2}$, $k_0=2\pi/\lambda_0$ is the wave number in vacuum, and $\eta=q_{1x}\varepsilon_2/(q_{2x}\varepsilon_1)$. When the wavelength is much longer than both the period d and the skin depth of metal (so that the field variation can be neglected in each layer), the periodic structure can be viewed as an effective medium. The effective dielectric constant is given by[7–9]

$$\varepsilon_e = \mathrm{diag}(\varepsilon_x, \varepsilon_y, \varepsilon_z), \quad (2)$$

$$\varepsilon_z = \varepsilon_y = f_1\varepsilon_1 + f_2\varepsilon_2, \quad (3)$$

$$\varepsilon_x = (f_1/\varepsilon_1 + f_2/\varepsilon_2)^{-1}, \quad (4)$$

where $f_1=d_1/d$ and $f_2=d_2/d$ are the filling fractions of metal and dielectric, respectively. The dispersion of p waves can be shown as

$$\frac{k_x^2}{\varepsilon_z} + \frac{k_z^2}{\varepsilon_x} = k_0^2. \quad (5)$$

In the following, we focus on a periodic Ag-air stratified structure with $d_1=10$ nm and $d_2=90$ nm. Experimental values are adopted for the dielectric constant of Ag.[26] Since Ag has almost the lowest optical loss among metals, the results

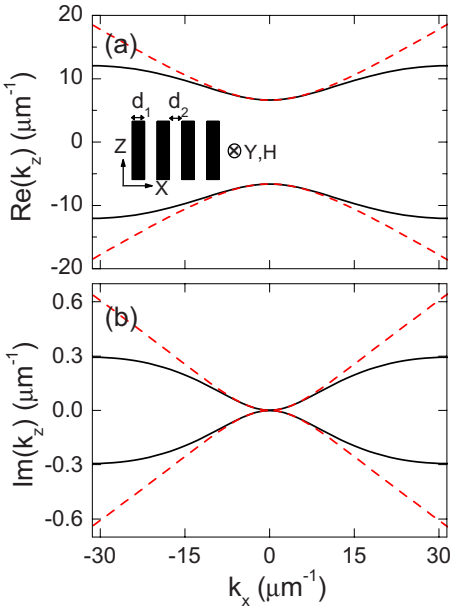

FIG. 1. (Color online) (a) Re(k_z) and (b) Im(k_z) as functions of k_x for p-polarized EM waves with wavelength of 1 μm in a periodic Ag-air stratified structure. The thicknesses of Ag and air layers are $d_1=10$ nm and $d_2=90$ nm, respectively. The solid and dashed lines are the results for the real structure [by Eq. (1)] and corresponding effective medium [by Eq. (5)], respectively.

of absorption will be better if other metals are applied. Figure 1 shows the equifrequency curve for the structure at wavelength of 1 μm. The solid lines are the accurate results calculated by TMM [Eq. (1)] and the dashed lines are the approximated ones by the effective-medium theory [Eq. (5)]. It can be seen that the difference is small between the two methods when $k_x < \pi/2d$. When $k_x=0$, the wave has a k_z close to k_0[Re(k_z/k_0)=1.05, $k_0=6.28$ μm^{-1}] and thus can be easily coupled with the wave in air. However, such a wave has a tiny loss [Im(k_z/k_0)=0.00013]. With increasing k_x, the waves suffer larger loss [e.g., when $k_x=\pi/d$ and $k_z=(12.0+0.29i)$ μm^{-1}] but have a lower coupling efficiency with the waves in air.

To improve the absorption for EM waves in air, we place the Ag-air stratified structure on a slanted Ag reflector as shown in Fig. 2(a). The reflector has an angle 45° to the z axis. When a EM wave is normally incident on the structure, the Bloch wave with $k_x=0$ can be excited and then be reflected into a wave with much larger loss. At the slanted mirror, the parallel wave vector should be equal for the reflected and incident Bloch waves, i.e., $k_{ix'}=k_{rx'}$. Using Eq. (1), the incident and reflected wave vectors are calculated from 0.5 to 4 μm as shown in Fig. 3. We can see that the incident wave vector is very close to k_0 and thus can be easily coupled with the light in air. The reflected wave has a large loss where Im(k_{rz}) is higher than 100 times of the incident one. The reflected Im(k_z) can even be 350 times of the incident one at wavelength of 1 μm[$k_{rz}=(9.6+0.27i)$ μm^{-1}, $k_{rx}=(16+0.27i)$ μm^{-1}].

To verify the predicted absorption enhancement, a finite-element method (COMSOL Multiphysics) is applied to do full-wave simulation for the structure in Fig. 2(a). Convergent results are obtained by increasing the number of grids. Figure 2(b) illustrates the field distribution for normal incidence of a Gaussian p wave with wavelength of 1 μm onto the structure. We can see that interference between the incident and reflected waves exists only near the Ag mirror. This indicates that the reflected waves are decaying from the mir-

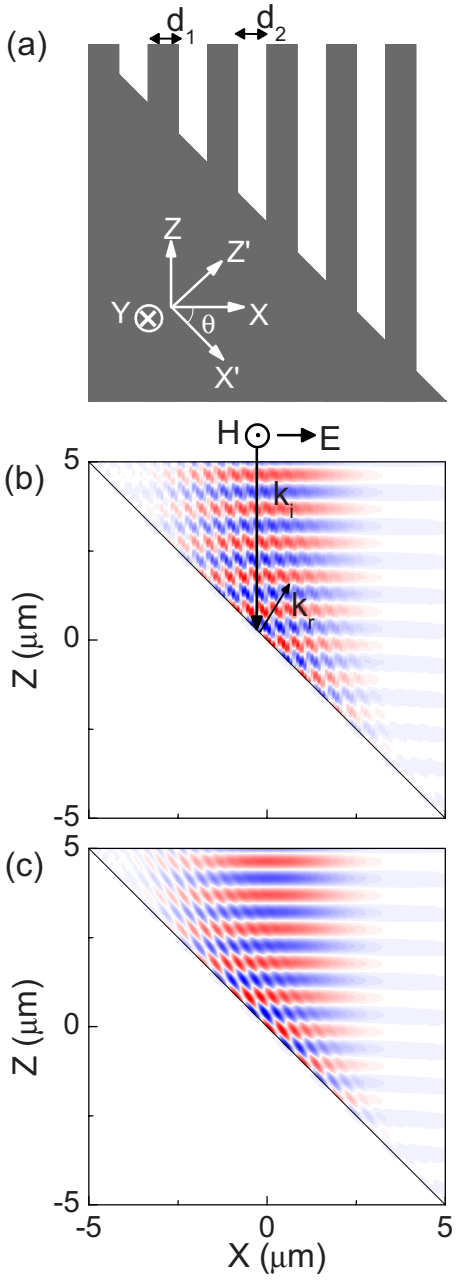

FIG. 2. (Color online) (a) Schematic of a periodic Ag-air stratified structure on a slanted Ag surface. The structure is invariant in the y direction. The angle between the Ag layers and the slanted surface $\theta=45°$. The thicknesses of Ag and air layers are $d_1=10$ nm and $d_2=90$ nm, respectively. (b) Finite-element simulation of normal incidence of a p-polarized Gaussian beam with wavelength of 1 μm from air onto the structure in (a). Red, white, and blue represent positive, zero, and negative values of H field, respectively. (c) The same as (b) but with using an effective medium to replace the Ag-air stratified structure.

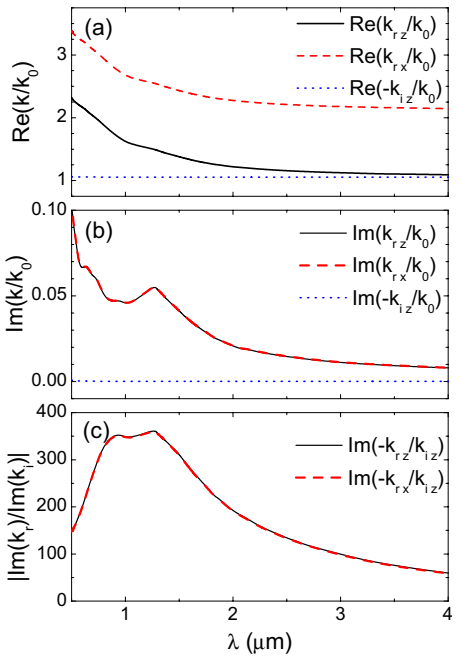

FIG. 3. (Color online) (a) $\mathrm{Re}(k/k_0)$, (b) $\mathrm{Im}(k/k_0)$, and (c) $\mathrm{Im}(k_r)/\mathrm{Im}(k_i)$ as functions of wavelength for the incident and reflected waves at the slanted Ag surface shown in Fig. 2.

ror, consistent with the above theoretical predictions $(\mathrm{Im}(k_{rx,z})^{-1}=3.7\ \mu\mathrm{m})$. Similar results are found if the stratified structure is replaced by an effective medium [Fig. 2(c)]. The reflected wave decays more rapidly due to the larger $\mathrm{Im}(k)$ from the effective-medium theory [Fig. 1(b)].

By integrals of power flow, we can obtain the reflection of a structure and the absorption for any part of the structure. The absorption is very low (5%) for a 5.5 μm thickness of Ag-air stratified structure. However, when the stratified structure is placed on a slanted Ag reflector, the absorption can be enhanced by about 20 times ($A=99\%$). 96% of the light is found to be absorbed by the stratified structure and the absorption of the flat Ag mirror is very small (3%). This indicates that the absorption enhancement is not related to surface waves and thus can occur in a broad frequency range. We also calculated the absorption for other wavelengths and found similar absorption enhancement.

The above process can be applied to realize broadband high absorption providing a large Ag reflector and thick stratified structure. To reduce the thickness of the whole structure, we place the AMM on a corrugated metallic surface as shown in Fig. 4(a). The corrugated surface is composed of a periodic array of isosceles ridges. In principle, if the ridges have smaller vertex angles and longer sides, the absorption of the structure will be higher. Here we focus on the case with a vertex angle of 90°. Such an aspect ratio (height/base=0.5) may ease the difficulties in fabrications. We first consider a corrugated surface with ridge height $h=5\ \mu$m. Other parameters are $t_1=t_2=0.5\ \mu$m [defined in Fig. 4(a)]. Figure 5 shows the absorption spectra of the structure from 0.5 to 4 μm at normal incidence (thick solid line). For comparison, the absorption spectra are also calculated for a stratified structure with 5.5 μm in thickness, the corrugated Ag surface, and a flat Ag film. It can be seen that the absorption is small (<0.1) for the flat Ag film (thin solid line). By introducing moderate surface oscillations (dashed line) or thin stratified structures (dotted line), the absorption can be enhanced but remains low. However, when the Ag-air stratified structure is placed on the corrugated Ag surface, the absorption can be enhanced by about 20 times due to the mechanism shown in Fig. 2.

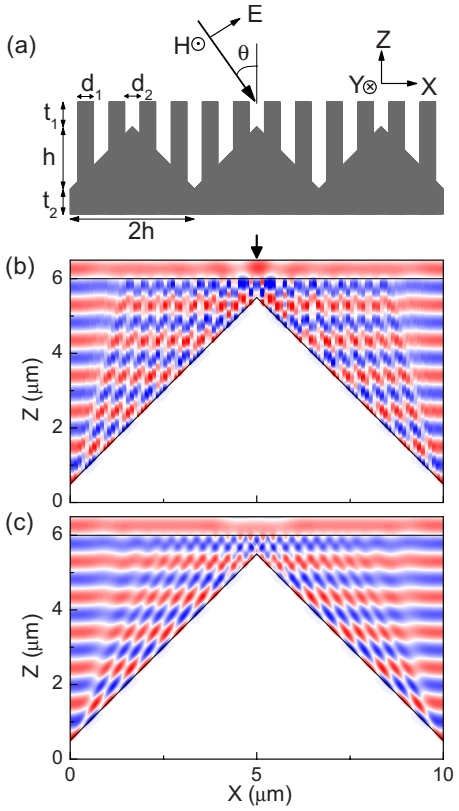

FIG. 4. (Color online) (a) Schematic of a periodic Ag-air stratified structure on a corrugated Ag film. The structure is invariant in the y direction. The thicknesses of Ag and air layers are $d_1=10$ nm and $d_2=90$ nm, respectively. The corrugated surface has a period $2h=10\ \mu$m and height $h=5\ \mu$m. $t_1=t_2=0.5\ \mu$m. (b) Finite-element simulation of normal incidence of a p-polarized plane wave with wavelength of 1 μm from air onto the structure in (a). Red, white, and blue represent positive, zero, and negative values of H field, respectively. The regions of $0<z<6\ \mu$m and $z>6\ \mu$m correspond to the Ag structure and air, respectively. (c) The same as (b) but with using an effective medium to replace the Ag-air stratified structure.

To see the light absorption more clearly, the magnetic field distribution is plotted in Fig. 4(b) at the wavelength of 1 μm. Compared with Fig. 2(b), the field is stronger in the vicinity of the vertex. This may be caused by the reflection of the vertex in the z direction. Hence, the absorption cannot be perfect but remains high in a wide frequency range ($A>87\%$ for $0.5\ \mu\mathrm{m}<\lambda<3\ \mu\mathrm{m}$). Similar results are found if the stratified structure is replaced by an effective medium [Fig. 4(c)]. The differences are that the reflected wave decays more rapidly and the field becomes more smoothly.

Figure 6 shows the absorption spectra of the above structure at oblique incidences ($\theta=30°, 45°, 60°$). It can be seen

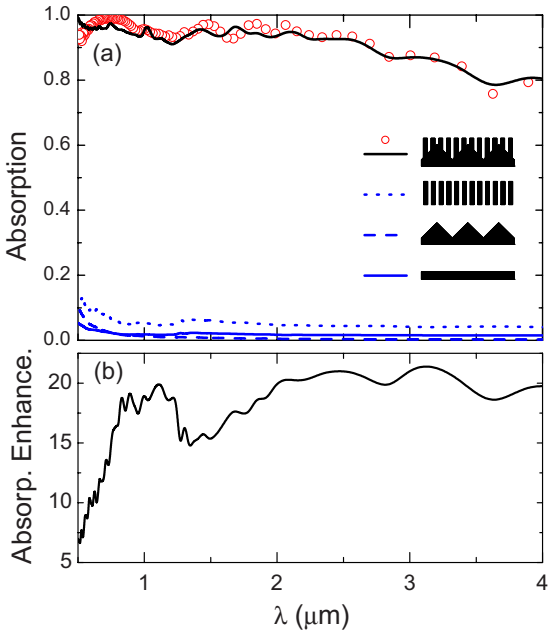

FIG. 5. (Color online) (a) Absorption spectra at normal incidence for four different Ag structures: the structure shown in Fig. 4(a) (black solid line and red/gray circles), a 5.5 μm height of the structure shown in the inset to Fig. 1(a) (dotted line), the corrugated Ag film shown in Fig. 4(a) (dashed line), and a Ag film with thickness 0.5 μm (blue/dark gray line). The red/gray circles are calculated by using an effective medium to replace the Ag-air stratified structure. (b) Absorption enhancement defined by the ratio of the absorption of the black solid line to that of the dotted line.

that in a wide range of angle ($|\theta|<45°$), the absorption is very close to the value at normal incidence. Even at $\theta=60°$, high absorption of 70% can still be found. An absorption dip appears at wavelength of 0.5 μm for $\theta=45°$. This dip becomes deeper and shifts a shorter wavelength with increasing

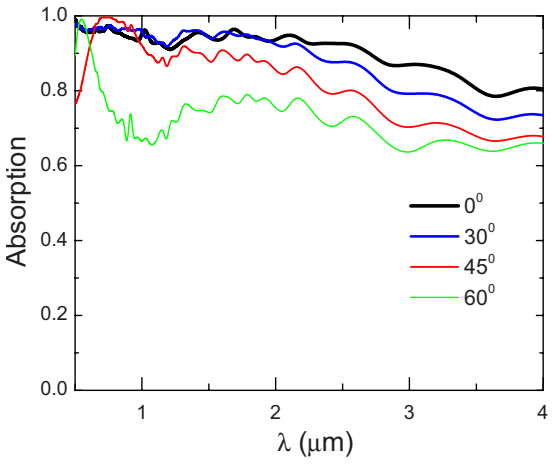

FIG. 6. (Color online) Absorption spectra for the Ag structure shown in Fig. 4(a) at different incident angles.

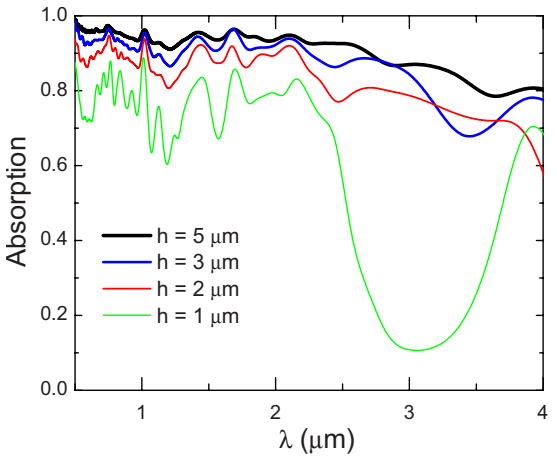

FIG. 7. (Color online) Absorption spectra at normal incidence for the Ag structure shown in Fig. 4(a) with different heights.

the incident angle. By calculating the reflection spectra of an infinitely thick Ag-air stratified structure, we found that this absorption dip is due to a partial reflection of *p*-polarized waves at interface between the stratified structure and air. The *s*-polarized waves can be reflected totally above a cutoff wavelength. The cutoff wavelength of *s* waves is found coincident with the reflection peak of *p* waves with varying the filling fraction of metal and incident angle. We note that the cutoff wavelength is longer than $2d_2$ since metal in optical wavelengths cannot be viewed as perfect metal. So the absorption dip at 0.5 μm in Fig. 6 is indeed a resonance phenomenon related to the cutoff wavelength.

The ridge height of the corrugated surface h is a critical parameter in our design. In Fig. 7, the absorption spectra are plotted for absorbers with $h=1,2,3,5$ μm and normal incidence. When h decreases, the absorption becomes lower due to the vertex effect. But if $h>2$ μm, favorable absorption ($A>85\%$ when 0.5 μm$<\lambda<2$ μm) can still be achieved. Some oscillations occur at the absorption curves. We found that for $h>3$ μm, the peak frequencies can be determined by the period of the corrugated surface ($f=m\pi/2h$, where m is an integer). But when h is small, the absorption becomes lower and other effects contribute to the peaks.

In summary, we have proposed that mirror reflections can be applied to enhance the absorption in anisotropic metamaterials. Using a thin MM of anisotropic ε_e situated on a corrugated Ag mirror, high absorption of *p* waves has been shown in a broad frequency range and over wide angular range. If a MM with anisotropic μ_e is provided, similar results should be obtained for *s* waves by using mirror reflections. Our results could have potential applications in solar cells and sensors. Extension of our results to acoustics will also be interesting.

This work was supported by the 973 Program (Grants No. 2007CB613200 and No. 2006CB921700) NSFC and the Shanghai Science and Technology Committee (Grants No. 09PJ1402000 and No. 08dj1400302).

*Corresponding author; huxh@fudan.edu.cn

[1] For a recent review, see D. R. Smith, J. B. Pendry, and M. Wiltshire, Science **305**, 788 (2004).
[2] J. B. Pendry, A. J. Holden, D. J. Robbins, and W. J. Stewart, IEEE Trans. Microwave Theory Tech. **47**, 2075 (1999).
[3] R. A. Shelby, D. R. Smith, and S. Schultz, Science **292**, 77 (2001).
[4] V. G. Veselago, Sov. Phys. Usp. **10**, 509 (1968).
[5] J. B. Pendry, Phys. Rev. Lett. **85**, 3966 (2000).
[6] D. R. Smith and D. Schurig, Phys. Rev. Lett. **90**, 077405 (2003).
[7] D. J. Bergman, Phys. Rep. **43**, 377 (1978).
[8] P. A. Belov and Y. Hao, Phys. Rev. B **73**, 113110 (2006).
[9] X. Li, Z. Liang, X. Liu, X. Jiang, and J. Zi, Appl. Phys. Lett. **93**, 171111 (2008).
[10] P. Halevi, A. A. Krokhin, and J. Arriaga, Phys. Rev. Lett. **82**, 719 (1999).
[11] X. Hu, C. T. Chan, J. Zi, M. Li, and K. M. Ho, Phys. Rev. Lett. **96**, 223901 (2006).
[12] D. Artigas and L. Torner, Phys. Rev. Lett. **94**, 013901 (2005).
[13] Z. Jacob, L. V. Alekseyev, and E. Narimanov, Opt. Express **14**, 8247 (2006).
[14] A. Salandrino and N. Engheta, Phys. Rev. B **74**, 075103 (2006).
[15] Z. W. Liu, H. Lee, Y. Xiong, C. Sun, and X. Zhang, Science **315**, 1686 (2007).
[16] U. Leonhardt, Science **312**, 1777 (2006).
[17] J. B. Pendry, D. Schurig, and D. R. Smith, Science **312**, 1780 (2006).
[18] D. Schurig, J. J. Mock, B. J. Justice, S. A. Cummer, J. B. Pendry, A. F. Starr, and D. R. Smith, Science **314**, 977 (2006).
[19] W. Cai, U. K. Chettiar, A. V. Kildishev, and V. M. Shalaev, Nat. Photonics **1**, 224 (2007).
[20] Y. Lai, H. Chen, Z. Q. Zhang, and C. T. Chan, Phys. Rev. Lett. **102**, 093901 (2009).
[21] N. I. Landy, S. Sajuyigbe, J. J. Mock, D. R. Smith, and W. J. Padilla, Phys. Rev. Lett. **100**, 207402 (2008).
[22] For a conventional absorber with a Fabry-Pérot cavity, see, e.g., X. Hu, M. Li, Z. Ye, W. Y. Leung, K. M. Ho, and S. Y. Lin, Appl. Phys. Lett. **93**, 241108 (2008).
[23] See, e.g., Z. P. Yang, L. Ci, J. A. Bur, S. Y. Lin, and P. M. Ajayan, Nano Lett. **8**, 446 (2008).
[24] P. Yeh, *Optical Waves in Layered Media* (Wiley, New York, 1988).
[25] J. Zi, J. Wan, and C. Zhang, Appl. Phys. Lett. **73**, 2084 (1998).
[26] *Handbook of Optical Constants of Solids*, edited by E. D. Palik (Academic, Orlando, 1985).